

Quantifying Stratospheric Ozone in the Upper Troposphere with In Situ Measurements of HCl

T. P. Marcy,^{1,2*} D. W. Fahey,^{1,2} R. S. Gao,¹ P. J. Popp,^{1,2}
E. C. Richard,^{1,2} T. L. Thompson,¹ K. H. Rosenlof,¹ E. A. Ray,^{1,2}
R. J. Salawitch,³ C. S. Atherton,⁴ D. J. Bergmann,⁴ B. A. Ridley,⁵
A. J. Weinheimer,⁵ M. Loewenstein,⁶ E. M. Weinstock,⁷
M. J. Mahoney³

We have developed a chemical ionization mass spectrometry technique for precise in situ measurements of hydrochloric acid (HCl) from a high-altitude aircraft. In measurements at subtropical latitudes, minimum HCl values found in the upper troposphere (UT) were often near or below the detection limit of the measurements (0.005 parts per billion by volume), indicating that background HCl values are much lower than a global mean estimate. However, significant abundances of HCl were observed in many UT air parcels, as a result of stratosphere-to-troposphere transport events. We developed a method for diagnosing the amount of stratospheric ozone in these UT parcels using the compact linear correlation of HCl with ozone found throughout the lower stratosphere (LS). Expanded use of this method will lead to improved quantification of cross-tropopause transport events and validation of global chemical transport models.

Ozone (O_3) that is produced in the stratosphere and transported into the upper troposphere (UT) is a substantial but uncertain contribution to the tropospheric O_3 budget (1–5). The increase in tropospheric O_3 in the industrial era is a key term in the radiative forcing of climate change (1, 2). A variety of chemical transport models (CTMs) predict a range of total stratosphere-to-troposphere O_3 transport that varies by more than a factor of 3 on a global annual basis (1, 3). The development of an accurate description and quantification of stratosphere-to-troposphere transport in CTMs will be required before an adequate accounting can be made of present and future UT O_3 abundances. No experimental technique has been able to reliably quantify stratospheric O_3 in the UT, particularly if significant mixing has occurred with background tropospheric air.

Long-lived gases (tracers) and correlations between tracers are often used to identify air parcels that have recently crossed the tropopause and to bound the net flux into the troposphere and stratosphere of O_3 and other gases (6–15). However, results from studies with tracers such as carbon monoxide (CO) or beryllium-7 to identify stratospheric O_3 in UT air parcels have been limited generally to being “semiquantitative” (6–9). The limitations arise in part from variable tropospheric sources of the tracer or from the lack of a known, compact, and linear correlation of the tracer with O_3 in the lower stratosphere (LS). Here we demonstrate the suitability of HCl as a quantitative tracer of stratospheric O_3 in the UT, using subtropical in situ measurements made over the United States in the summer of 2002.

HCl has four attributes that underlie the quantification of stratospheric O_3 in the UT and that, as a group, are not shared by any other tracer currently being measured in situ or remotely. These attributes are as follows:

1) HCl has no known, significant sources in the UT, nor is the abundance of HCl expected to be significant in the UT, apart from what is transported from the stratosphere. However, short-lived organic species transported from the surface may be a source under some conditions (16). There are important sources of HCl in the lower troposphere (17, 18), but wet scavenging of HCl in clouds

makes it unlikely that appreciable amounts of HCl reach the UT. The lack of a significant upper tropospheric source is an important attribute, because such a source would create ambiguity as to the origin of HCl observed in the UT.

2) HCl (as well as O_3) has a photochemical lifetime on the order of weeks in the UT and LS (supporting online material), due in part to low ultraviolet fluxes and the long lifetimes of the primary halocarbon source molecules for HCl. With a long lifetime, HCl will remain a good tracer of LS O_3 present in the UT until precipitation scavenging results in selective HCl removal from an air parcel.

3) HCl has a compact, linear correlation with O_3 throughout the LS. The correlation occurs because HCl is produced in the middle and upper stratosphere in approximately the same region where O_3 is produced. The linearity of the correlation is the result of the long photochemical lifetimes of HCl and O_3 and of the transport and mixing that occurs in the LS away from the production region (10, 11). A linear correlation is needed in the LS in order to define and minimize the uncertainty in the quantification of stratospheric O_3 in the UT.

4) On the basis of our results, HCl can be measured in situ with high precision [0.005 parts per billion by volume (ppbv)] and high spatial resolution (<1 km). This precision allows stratospheric O_3 amounts as low as 11 ppbv to be detected in the UT.

We measured HCl using a chemical ionization mass spectrometry (CIMS) instrument (19, 20) that was flown on the NASA WB-57F high-altitude aircraft in July 2002. On the flights of 29 and 31 July (hereafter referred to as Flt. A and Flt. B, respectively), the CIMS was operated with a new ion chemistry scheme based on the SF_5^- reagent ion. The SF_5^- scheme was developed to obtain sensitive and selective measurements of HCl, HNO_3 , and $ClONO_2$ in the atmosphere (supporting online material). The detection limit for HCl was 0.005 ppbv (1 s, 1σ), with an overall accuracy of $\pm 25\%$ for values above the detection limit. Many other measurements were made simultaneously on board the aircraft. Those used here include O_3 , tropopause height, total reactive nitrogen (NO_y), CO, water vapor (H_2O), condensation nuclei, and potential temperature (21). The observations were compared to results from a three-dimensional global CTM, the Integrated Massively Parallel Atmospheric Chemical Transport (IMPACT) model (3) (supporting online material).

HCl in the stratosphere. Correlations of the HCl and O_3 measurements from Flts. A and B were plotted for altitudes between 11

¹Aeronomy Laboratory, National Oceanic and Atmospheric Administration, Boulder, CO 80305, USA. ²Cooperative Institute for Research in Environmental Sciences, University of Colorado, Boulder, CO 80309, USA. ³Jet Propulsion Laboratory, California Institute of Technology, Pasadena, CA 91109, USA. ⁴Atmospheric Science Division, Lawrence Livermore National Laboratory (LLNL), Livermore, CA 94550, USA. ⁵National Center for Atmospheric Research, Boulder, CO 80307, USA. ⁶NASA Ames Research Center, Moffett Field, CA 94035, USA. ⁷Harvard University, Cambridge, MA 02138, USA.

*To whom correspondence should be addressed. E-mail: tmarcy@al.noaa.gov

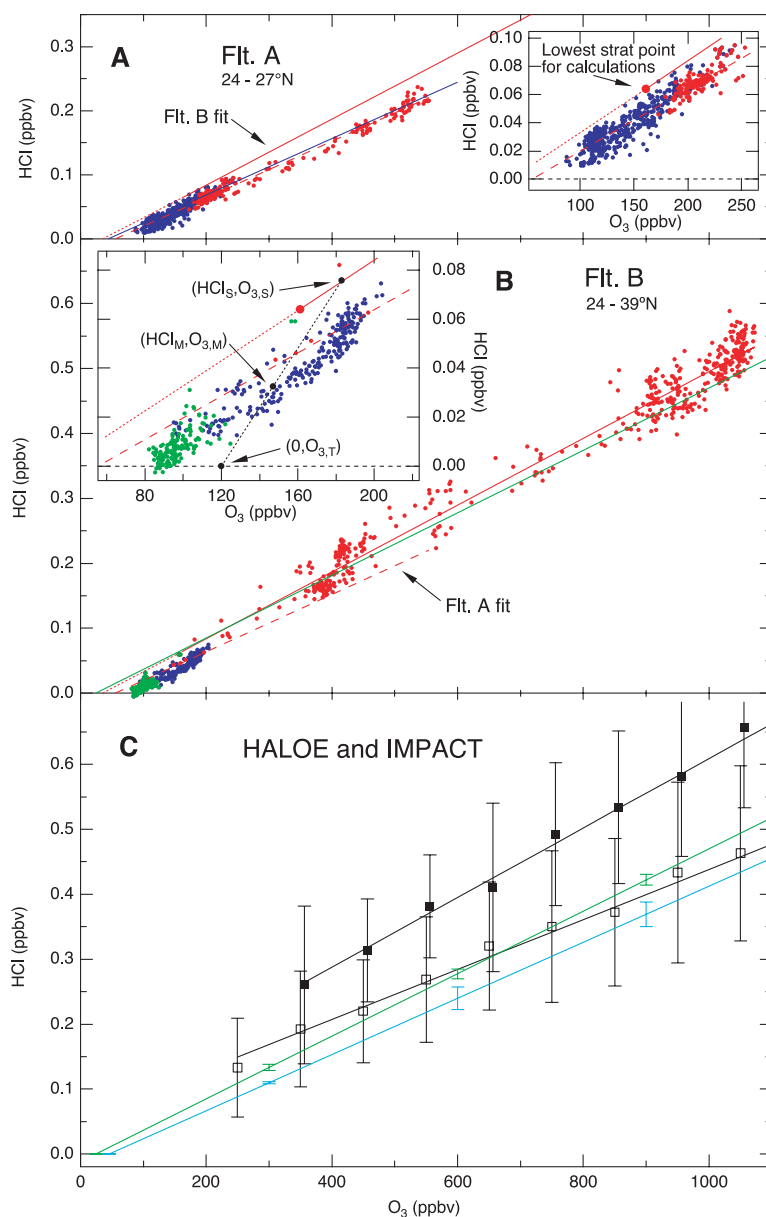
and 18 km, for latitudes between 24°N and 39°N (Fig. 1). The HCl:O₃ correlations are compact and linear in the LS and extend into the UT for both flights. Linear fits are shown for the stratospheric data from each flight. The linear correlations in the LS, which are expected based on the long lifetime of each gas, are produced by effective mixing between end-member air parcels (10, 11). The most extreme end members in this overall mixing process are located in the LS near the tropopause and at altitudes well above the LS observation region. End-member air parcels near the tropopause are formed, in part, from tropospheric air containing low O₃ (<200 ppbv) and low HCl, and entering the stratosphere primarily from low latitudes (<30°) (22–24). Differing amounts of tropospheric O₃ in the air that enters the LS will result in

small differences in the O₃ intercepts of the extrapolated LS correlations. We found small intercept differences between Flts. A and B (Fig. 1, insets). The differences in the LS correlation slopes between the two flights are consistent with the latitude dependence found in other observations and our model results.

The IMPACT model includes explicit treatment of chemistry and transport processes in the LS. The LS correlations in the model runs for late July 2002 show low variability at latitudes of 26°N and 46°N (Fig. 1C). These correlations include tropospheric values of O₃, because results are shown for altitudes above 9 km (~300 hPa). For comparison to the flight results, the IMPACT correlation fits are included in Fig. 1, A and B. The excellent agreement found for the LS portion provides essential validation of the full stratospheric simulation in IMPACT.

Previously unpublished HCl:O₃ correlations from the Halogen Occultation Experiment (HALOE) satellite data set (25) (Fig. 1C) also show that a linear correlation between HCl and O₃ is ubiquitous in the LS. This data set, as well as the IMPACT results, shows a weak latitude dependence of the slope (supporting online material). HCl in the UT/LS region has also been measured in situ (26, 27) and remotely by instruments on balloons (28) and the space shuttle (27). None of these data sets has been used to examine the HCl:O₃ correlation in the UT/LS or LS-to-UT transport. The HALOE data set stands out among the previous data sets because of its global coverage over more than a decade. The linear fits to the HALOE data are offset (to higher HCl or lower O₃) with respect to both the IMPACT model results and the in situ observations (supporting online material).

Fig. 1. Correlations of measured and modeled mixing ratios of HCl and O₃. **(A and B)** Data acquired on two flights during the NASA Cirrus Regional Study of Tropical Anvils and Cirrus Layers–Florida Area Cirrus Experiment (CRYSTAL-FACE) mission during July 2002. Both were 5-hour flights that sampled the UT/LS region up to altitudes near 18 km (200 to 70 hPa). Aircraft data points are divided into groups for the stratosphere (red) and troposphere (green and blue). The distinction between tropospheric and stratospheric data is based on thermal tropopause height measured by remote temperature sounding on board the aircraft. Insets show details of the tropospheric data. Red lines represent unconstrained linear fits to the stratospheric data from Flts. A (dashed) and B (solid) and have slopes of $(4.4 \pm 0.04) \times 10^{-4}$ and $(5.1 \pm 0.04) \times 10^{-4}$, respectively. The CIMS HCl data were acquired at a rate of ~8 Hz during 3 s of every 12-s interval. Data points are averages of each 3-s interval. A spatial resolution of 0.6 km follows from the aircraft speed of ~200 m s⁻¹. **(A)** Data from Flt. A, in the latitude range of 24°N to 27°N near Key West, FL. The blue line is a linear fit to the IMPACT model results near Key West (26°N, 280°E) from 15 July to 1 August 2002. Strat, stratospheric. **(B)** Data from Flt. B, which originated in Key West and covered latitudes from 24°N to 39°N before landing in Houston, TX (30°N). The blue points are tropospheric data from the first flight leg (near Key West), and the green points are tropospheric data from the second leg (near Houston). The green line is a linear fit to the IMPACT model results and is also shown in **(C)**. Inset: Details of the tropospheric data along with a hypothetical mixing line (dotted black line) that shows that an arbitrary air parcel ($\text{HCl}_{\text{M}}, \text{O}_{3,\text{M}}$) can be formed from mixing between two other air parcels: the stratospheric end member ($\text{HCl}_{\text{S}}, \text{O}_{3,\text{S}}$) and the tropospheric end member ($0, \text{O}_{3,\text{T}}$). The larger red point on the Flt. B fit line in the insets indicates the lowest stratospheric point used in the calculation of the stratospheric O₃ fraction. **(C)** Results from the HALOE satellite and the IMPACT model. The HALOE data are from the month of July for each of the years 1993 to 2003, for pressures between 83 and 35 hPa. The data were filtered to remove retrievals with anomalously high methane values (>1650 ppbv) that skew the retrieved HCl values (25). The data are binned in 100-ppbv O₃ intervals, and black error bars give the standard deviations in each bin. The black lines are linear fits to the HALOE data between 20°N and 50°N [black squares, slope of $(5.4 \pm 0.17) \times 10^{-4}$] and between 20°S and 20°N [open squares, slope of $(3.9 \pm 0.15) \times 10^{-4}$]. The IMPACT results are averages from 29 July to 1 August, 2002, at latitudes of 26°N (blue line) and 46°N (green line) and longitudes between 255°E and 285°E. The error bars on the IMPACT fit lines are standard deviations for selected 100-ppbv O₃ bins. Only model results from altitudes >9 km (300 hPa) and with <600 or <1000 ppbv O₃ are included, for consistency with the data from Flts. A and B, respectively. The model slopes are $(4.30 \pm 0.01) \times 10^{-4}$ and $(4.81 \pm 0.01) \times 10^{-4}$ for 26°N and 46°N, respectively.



HCl in the troposphere. Significant amounts of HCl were present in tropospheric air parcels (Fig. 1, green and blue data points). The tropopause height along the flight track, which is used to distinguish tropospheric from stratospheric air, is derived from temperature soundings made on board the aircraft (21, 29). Two features of the tropospheric data are apparent. First, many air parcels have minimum HCl values that are at or near the detection limit of 0.005 ppbv, implying that background HCl is very low in the UT. Average HCl for part of Flt. B (Fig. 1, green points) is particularly notable because average HCl is 0.007 ± 0.005 ppbv, over a horizontal distance of 300 km at an altitude of 14 km. These observations alone suggest that large regions of the UT generally will have HCl values much lower than 0.1 ppbv, which is a current budget estimate for average free-tropospheric HCl (17). For our lowest HCl values (<0.02 ppbv), the associated O_3 values were less than 150 ppbv, which is consistent with values expected from ozone sonde climatologies for the background UT (30). The second data feature is that the HCl: O_3 correlations in the tropospheric data set are compact and essentially linear in both flights, with slopes comparable to the LS correlations. These compact correlations provide strong evidence that the UT HCl values, which range up to nearly 0.1

ppbv, result from the transport of substantial amounts of stratospheric air and O_3 into the UT. In addition, the fact that no UT data points fall above the extrapolated stratospheric fit line is a further indication of the absence of a substantial HCl source in the background UT, other than transport from the stratosphere.

The IMPACT results (Fig. 1C) also show that the HCl: O_3 compact correlation extends below the tropopause (~ 200 ppbv O_3) and that low values (<0.02 ppbv) of HCl are reached. The minimum model HCl values reached in the observational area near Florida were <0.005 ppbv. These UT model features are highly consistent with those found in the observations. IMPACT uses a constant surface mixing ratio for HCl of 0.085 ppbv to simulate the surface source. Vertical profiles of HCl previously measured in the troposphere show elevated concentrations (up to 0.5 ppbv) near the surface, due to localized sources, and much lower levels (near 0.05 ppbv) at the 7-km upper limit of the measurements (18). We conducted a separate IMPACT simulation in which we evaluated the contribution of surface HCl to the free troposphere by doubling the imposed surface HCl mixing ratio. The resulting change in HCl in the UT was negligible (31). This test indicates that wet deposition is very effective in the model in preventing surface HCl from reaching the UT.

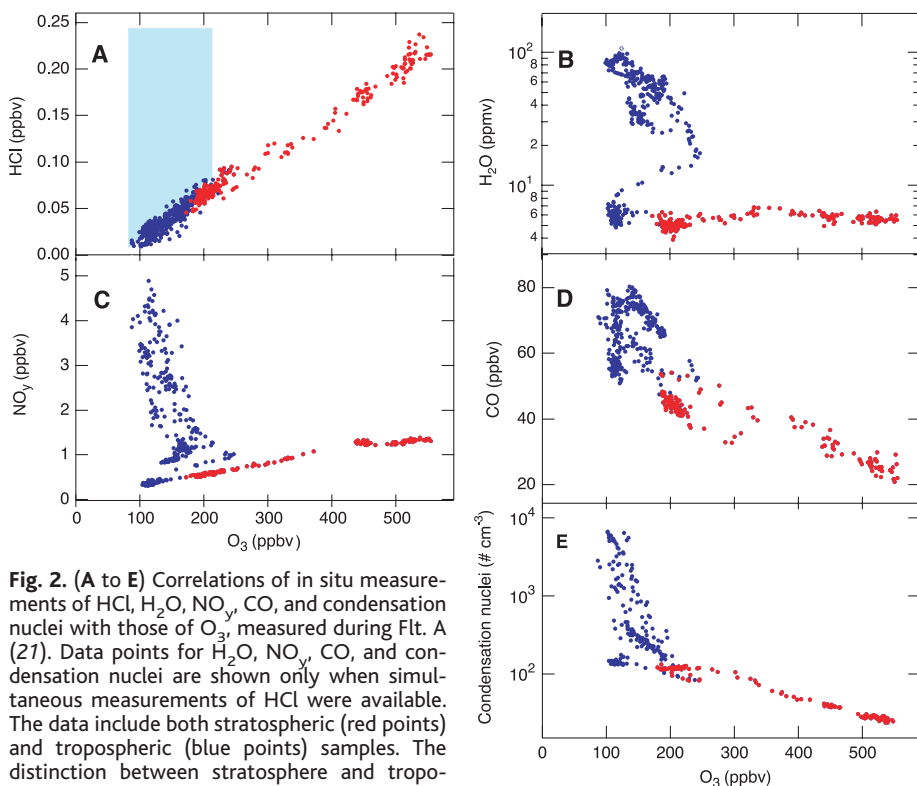


Fig. 2. (A to E) Correlations of in situ measurements of HCl, H_2O , NO_y , CO, and condensation nuclei with those of O_3 , measured during Flt. A (27). Data points for H_2O , NO_y , CO, and condensation nuclei are shown only when simultaneous measurements of HCl were available. The data include both stratospheric (red points) and tropospheric (blue points) samples. The distinction between stratosphere and troposphere data is based on the onboard remote sounding of the thermal tropopause height. The absence of data points in the shaded region of (A) is evidence of a negligible tropospheric background of HCl.

The HCl: O_3 correlation on Flt. A is contrasted with the correlations of O_3 with NO_y , CO, H_2O , and condensation nuclei (Fig. 2). Several important points follow from this comparison. First, these non-HCl tracers, which are routinely measured in situ, also show compact correlations with O_3 in the LS (and therefore also with HCl). In the UT, the compactness of these other correlations is greatly reduced, with non-HCl tracer values exceeding those found in the LS. These changes are a result of the highly variable tropospheric sources of NO_y , CO, H_2O , and condensation nuclei, which create large values and spatial gradients of these tracers in the UT that are unrelated to stratospheric intrusions. The changes in these non-HCl correlations exemplify, in part, why they cannot be used routinely to quantify stratospheric O_3 in the UT with useful accuracy. Second, the HCl: O_3 correlation contrasts sharply with those of the other tracers, showing essentially no change in compactness between the LS and UT. If significant HCl amounts were produced in the UT or transported from the surface to the UT, a less compact HCl: O_3 correlation plot would be expected in the UT, with data points that occur in the shaded region in Fig. 2A. Third, the contrast in the compactness of the UT correlations between HCl and the other tracers provides strong evidence that the UT parcels shown in Fig. 2 result from mixing of stratospheric and tropospheric air; hence, the contrast also provides evidence that the transport of LS air to the UT is irreversible in this case. Finally, the compact LS correlations of the non- O_3 tracers with HCl, as implied by the data in Fig. 2, could also be used to quantify stratospheric abundances of these non- O_3 tracers in the UT in a manner similar to that described below for O_3 .

Quantifying stratospheric O_3 in the UT. When HCl measurements are used to quantify the amount of stratospheric O_3 transported to the UT or mixed into UT air parcels, two key assumptions are required. First, the HCl/ O_3 ratio is conserved during transport of stratospheric air into the UT. This follows from the long photochemical lifetimes of both tracers and the general absence of wet scavenging of HCl in stratosphere-troposphere exchange events in the UT. Second, in the UT parcels under consideration, the amount of HCl from nonstratospheric sources is negligible in comparison to that transported from the LS. Here, the definition of stratospheric O_3 in the UT is O_3 that has recently been above the thermal tropopause (29).

Based on these assumptions, the amount of stratospheric O_3 in a UT parcel can be expressed as

$$\text{Stratospheric } [O_3] = [HCl_M] \cdot [O_{3,S}] / [HCl_S]$$

(1)

where brackets indicate abundance, $[HCl_M]$ is the measured HCl in the UT parcel, and $[O_{3,S}]/[HCl_S]$ is the ratio of O_3 to HCl in the air parcel(s) that are the source of the stratospheric O_3 . This expression reflects the fact that HCl-containing air parcels sampled in the UT are, in general, the result of a multi-stage mixing process between parcel(s) of stratospheric air and parcel(s) of background tropospheric air (Fig. 1) (supporting online material). The origin of the stratospheric air in a particular UT parcel influences the choice of the $[O_{3,S}]/[HCl_S]$ ratio used in Eq. 1 for that parcel. For example, meteorological trajectory analysis for Flts. A and B shows that stratospheric air entered the troposphere over the Florida region throughout July through isentropic transport from higher latitudes (32). As a consequence, the average $[O_{3,S}]/[HCl_S]$ ratio of 2250 from Flt. B, the higher latitude flight, is chosen here to calculate the fraction of stratospheric O_3 for both flights. One source of uncertainty in the $[O_{3,S}]/[HCl_S]$ ratio is associated with the assumption of negligible background HCl in the UT. Although the observational and model results suggest that background HCl values as low as 0.005 ppbv are common in the UT, the true range and distribution of background values will not be known until more extensive observations are made. A background HCl value equal to the detection limit (0.005 ppbv) corresponds to a detection limit for stratospheric O_3 in Eq. 1 of 11 ppbv. Based in part on this background value, the overall

uncertainty in a stratospheric O_3 value is estimated as the sum of $\pm 15\%$ of the value and ± 11 ppbv (supporting online material).

The stratospheric O_3 fractions for Flts. A and B are shown as vertical profiles (Fig. 3). The UT data separate into two cases. The first case (Fig. 3, blue points) represents remnants of recent intrusions of mid-latitude stratospheric air into the UT above Florida. The fractions vary from 0.2 to 0.9, indicating a wide range of irreversible mixing of UT and LS air. The error bars are examples of the estimated uncertainties in the fraction. The second case (Fig. 3, green points) represents UT air far from the mid-latitude intrusions found over Florida, with fractions that vary over a narrower range, from 0.0 to 0.4. This group includes the 300-km (31°N to 33°N) flight segment, over which the average HCl amount was 0.007 ppbv. The vertical ranges in the two cases are also distinct. In the first, the intrusion affects several kilometers below the tropopause. In the second, the influence of stratospheric O_3 is negligible a kilometer below the tropopause. The IMPACT model also shows a UT disturbance over Florida (supporting online material) (fig. S1), which is nominally consistent with the large stratospheric O_3 values in the first case. Although the model results are limited by low vertical resolution, this comparison provides a first-order example of how to use in situ HCl observations to confirm stratosphere-to-troposphere exchange events and the accumulation of O_3 from such exchange in CTMs.

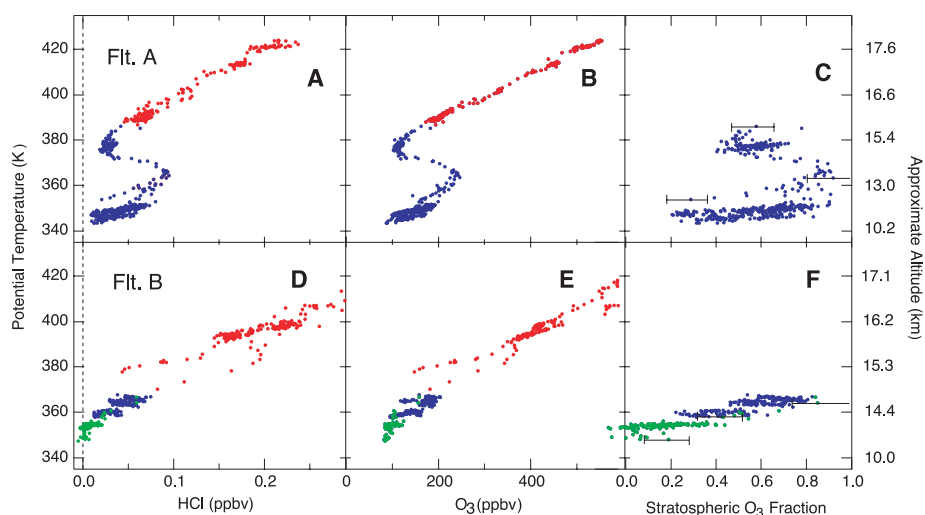


Fig. 3. Vertical profiles of measured HCl, O_3 , and the calculated stratospheric O_3 fraction for (A to C) Flt. A and (D to F) Flt. B. The data set is identical to that used in Fig. 1. Each profile is shown with calculated potential temperature (left axis) and the approximate corresponding altitude (right axis). Potential temperature is derived from onboard temperature and pressure measurements. Data are shown for the stratosphere (red points) and the troposphere (green and blue points). The blue points in (C) and (F) are affected by a stratospheric intrusion, caused by flow around a quasistationary anticyclone that was located over the south-central United States for most of the preceding month (33). The green points in (D), (E), and (F) are from the second leg of Flt. B (covering a horizontal distance of about 300 km between 33°N and 31°N and just more than 1 km below the tropopause) and correspond to the green points in Fig. 1B. The error bars in (C) and (F) are representative examples of the uncertainty in the calculated stratospheric O_3 fractions.

Quantifying stratospheric ozone in UT air parcels (as with Eq. 1) is distinct from, but related to, quantifying the amount of stratospheric air that is transported to the UT or mixed with UT air. A given amount of stratospheric O_3 in a UT air parcel can result from mixing with a small fraction of stratospheric air with high O_3 content or a larger fraction of stratospheric air with a lower O_3 content. Although the fraction of stratospheric air in a measured UT parcel cannot be determined from the HCl and O_3 measurements (because the particular stratospheric end members involved in the mixing are unknown), we can derive an upper limit by assuming that the stratospheric end-member parcel has the lowest observed value of O_3 , which is ~ 160 ppbv in this study. Values near this upper limit are more likely than lower values, because stratospheric parcels with the lowest O_3 values are near the tropopause and hence are more likely to be involved in cross-tropopause intrusion and mixing events.

Stratospheric HCl molecules irreversibly mixed into the UT will be lost from an air parcel after sufficient time through wet removal processes. Stratospheric O_3 molecules in the UT will participate in various photochemical cycles that might lead to their destruction. The independent loss of HCl and the production and removal of O_3 from UT parcels represent a limitation in the use of Eq. 1 for long periods after an exchange event (33).

The ability of CTMs to resolve O_3 transport to the UT has improved considerably in recent years (34, 35). For example, CTM analysis of the low-latitude UT shows large-scale intrusions of O_3 confirmed by lidar soundings (34). Direct comparisons of model results with estimates of stratospheric O_3 in the UT obtained with high-precision HCl observations, in addition to other tracer measurements, have great potential to describe fine- and large-scale details of the exchange process. These details will facilitate a resolution of the inconsistencies in global UT O_3 budgets regarding the stratospheric source (1). Our observations constrain the UT HCl budget and indicate that background values in large regions of the UT are much lower than published estimates. Global measurements of HCl and O_3 in the UT will facilitate meaningful tests of the representation of stratospheric intrusions in CTMs and will lead to improved estimates of HCl source strengths and transport and removal processes.

References and Notes

1. J. T. Houghton et al., Eds., *Climate Change 2001: The Scientific Basis* (Cambridge Univ. Press, New York, 2001).
2. M. Gauss et al., *J. Geophys. Res.* **108**, 10.1029/2002JD002624 (2003).
3. D. A. Rotman et al., *J. Geophys. Res.* **109**, 10.1029/2002JD003155 (2004).
4. F. C. Fehsenfeld, S. C. Liu, in *Global Atmospheric*

- Chemical Change*, C. N. Hewitt, W. T. Sturges, Eds. (Elsevier, New York, 1993), pp. 169–231.
5. A. Stohl et al., *J. Geophys. Res.* **108**, 10.1029/2002JD002490 (2003).
 6. H. Fischer et al., *Geophys. Res. Lett.* **27**, 97 (2000).
 7. P. Hoor, H. Fischer, L. Lange, J. Lelieveld, D. Brunner, *J. Geophys. Res.* **107**, 10.1029/2000JD000289 (2002).
 8. A. Zahn et al., *J. Geophys. Res.* **107**, 10.1029/2001JD001529 (2002).
 9. J. E. Dibb et al., *J. Geophys. Res.* **108**, 10.1029/2001JD001347 (2003).
 10. R. A. Plumb, M. K. W. Ko, *J. Geophys. Res.* **97**, 10145 (1992).
 11. R. A. Plumb, D. W. Waugh, M. P. Chipperfield, *J. Geophys. Res.* **105**, 10047 (2000).
 12. J. Lelieveld et al., *Geophys. Res. Lett.* **24**, 603 (1997).
 13. C. D. Nevison et al., *Global Biogeochem. Cycles* **13**, 737 (1999).
 14. D. M. Murphy, D. W. Fahey, *J. Geophys. Res.* **99**, 5325 (1994).
 15. C. M. Volk et al., *J. Geophys. Res.* **102**, 25543 (1997).
 16. C. A. Ennis, Ed., *Scientific Assessment of Ozone Depletion: 2002* [World Meteorological Organization (WMO), Geneva, 2003].
 17. T. E. Graedel, W. C. Keene, *Global Biogeochem. Cycles* **9**, 47 (1995).
 18. B. Vierkorn-Rudolph, K. Backmann, B. Schwarz, F. X. Meixner, *J. Atmos. Chem.* **2**, 47 (1984).
 19. J. A. Neuman et al., *Rev. Sci. Instr.* **71**, 3886 (2000).
 20. J. A. Neuman et al., *Atmos. Environ.* **35**, 5789 (2001).
 21. We measured O₃ by a fast-response, dual-beam, ultraviolet-absorption ozone photometer with an overall uncertainty of 5% (36). We measured NO_x with an NO/O₃ chemiluminescence instrument (37) with an overall uncertainty of ± (0.015 ppbv + 9%); H₂O with a Lyman-α photofragment fluorescence hygrometer (38) with an accuracy of ±10%; CO by tunable diode laser absorption with precision of ±7.4 ppbv; and condensation nuclei with a nucleation-mode aerosol size spectrometer (39) with a combined uncertainty of ±38%. The tropopause height was measured with a microwave temperature profiler (40) within an accuracy of 0.5 km. Temperature and pressure were measured with aircraft probes, with accuracies of 0.5 K and 0.5 hPa, respectively.
 22. J. R. Holton et al., *Rev. Geophys.* **33**, 403 (1995).
 23. A. F. Tuck et al., *Q. J. R. Meteorol. Soc.* **123**, 1 (1997).
 24. K. H. Rosenlof et al., *J. Geophys. Res.* **102**, 13213 (1997).
 25. J. M. Russell III et al., *J. Geophys. Res.* **101**, 10151 (1996).
 26. C. R. Webster et al., *J. Geophys. Res.* **105**, 11711 (2000).
 27. H. A. Michelsen et al., *Geophys. Res. Lett.* **26**, 921 (1999).
 28. G. C. Toon et al., *J. Geophys. Res.* **104**, 26779 (1999).
 29. A chemical or dynamical definition of the tropopause will give different, usually lower, tropopause heights than the thermal WMO definition (41). Here, the primary concern is to identify the stratospheric HCl/O₃ ratio. Because there will often be some tropospheric influence in the LS, choosing the highest commonly accepted tropopause value is the most reliable approach for determining the stratospheric HCl/O₃ ratio. Of the commonly used methods, the thermal tropopause has often been the highest value (41).
 30. J. A. Logan, *J. Geophys. Res.* **104**, 16115 (1999).
 31. The doubling of the IMPACT HCl surface boundary condition to 0.17 ppbv resulted in changes in the UT (pressure altitudes above 220 hPa) of less than 2% for much of the globe, with peak differences of 5 to 10%. The model results give HCl abundances of less than 0.01 ppbv for much of the global UT with either HCl surface value, because of the very low efficiency of transport of surface HCl to the UT and the lack of any local HCl source in the UT.
 32. E. C. Richard et al., *J. Geophys. Res.* **108**, 10.1029/2003JD003884 (2003).
 33. An estimate of the time before upper troposphere air mixes with lower tropospheric air is given by the turnover time of the tropical upper troposphere of ~10 days (42). The times might be longer for regions at higher latitudes away from convection.
 34. O. Wild et al., *J. Geophys. Res.* **108**, 10.1029/2002JD003283 (2003).
 35. D. A. Hauglustaine, G. P. Brasseur, *J. Geophys. Res.* **106**, 32337 (2001).
 36. M. H. Proffitt, R. L. McLaughlin, *Rev. Sci. Instrum.* **54**, 1719 (1983).
 37. B. A. Ridley et al., *J. Geophys. Res.* **99**, 25519 (1994).
 38. E. M. Weinstock et al., *Rev. Sci. Instrum.* **65**, 3544 (1994).
 39. J. C. Wilson, W. T. Lai, S. D. Smith, *J. Geophys. Res.* **96**, 17415 (1991).
 40. R. F. Denning, S. L. Guidero, G. S. Parks, B. L. Gary, *J. Geophys. Res.* **94**, 16757 (1989).
 41. S. Bethan, G. Vaughan, S. J. Reid, *Q. J. R. Meteorol. Soc.* **122**, 929 (1996).
 42. M. J. Prather, D. J. Jacob, *Geophys. Res. Lett.* **24**, 3189 (1997).
 43. We thank the pilots and crew of the NASA WB-57F for making the airborne measurements presented here possible, J. C. Wilson for use of condensation nuclei data, and L. L. Gordley and A. Stohl for helpful discussions. Partially supported by NASA's Upper Atmospheric Research Program and Radiation Science Program. Work at the Jet Propulsion Laboratory (R.J.S. and M.J.M.) was carried out under contract with NASA. Participation of LLNL authors occurred through the University of California under the auspices of the U.S. Department of Energy contract no. W-7405-ENG-48.

Supporting Online Material

www.sciencemag.org/cgi/content/full/304/5668/261/

DC1

SOM Text

Fig. S1

References and Notes

7 November 2003; accepted 11 March 2004

Functional Conversion Between A-Type and Delayed Rectifier K⁺ Channels by Membrane Lipids

Dominik Oliver,^{1*} Cheng-Chang Lien,^{1*} Malle Soom,²
Thomas Baukowitz,² Peter Jonas,^{1†} Bernd Fakler^{1†}

Voltage-gated potassium (Kv) channels control action potential repolarization, interspike membrane potential, and action potential frequency in excitable cells. It is thought that the combinatorial association between distinct α and β subunits determines whether Kv channels function as non-inactivating delayed rectifiers or as rapidly inactivating A-type channels. We show that membrane lipids can convert A-type channels into delayed rectifiers and vice versa. Phosphoinositides remove N-type inactivation from A-type channels by immobilizing the inactivation domains. Conversely, arachidonic acid and its amide anandamide endow delayed rectifiers with rapid voltage-dependent inactivation. The bidirectional control of Kv channel gating by lipids may provide a mechanism for the dynamic regulation of electrical signaling in the nervous system.

The action potential (AP) is the fundamental unit of information in the brain (1). Its shape is of critical importance in many forms of neuronal signaling (2–5). Voltage-gated potassium (Kv) channels shape the AP by controlling its repolarization phase and determine the membrane potential and duration of the interspike interval (I). Delayed rectifier Kv channels keep single APs short and permit high-frequency trains of APs (6). Rapidly inactivating A-type channels help a cell fire at low frequency (7) and promote broadening of APs during repetitive activity (6).

It is widely accepted that the functional properties of Kv channels are determined by their α - and β -subunits [Kv α families 1 to 4 (8) and Kv β families 1 to 3 (9)]. Most Kv α subunits encode delayed rectifier

channels with slow inactivation, whereas only a few exhibit A-type behavior (8). Inactivation is generated by two distinct mechanisms. One is the N-type (or ball-and-chain) inactivation, in which an N-terminal protein domain of certain Kv α or Kv β subunits plugs the open channel pore from the cytoplasmic side (10); the other is C-type inactivation, which appears to result from constriction or collapse of the channel's selectivity filter (11).

Membrane phospholipids and their metabolites are implicated in regulation of excitability and retrograde modulation at synapses (12, 13). Lipid molecules in plasma membranes regulate the gating of ion channel proteins. The phospholipid phosphatidylinositol-4,5-bisphosphate (PIP₂) modifies the gating of inward rectifier (Kir) K⁺ channels (14–16), KCNQ-type K⁺ channels (17), voltage-gated Ca²⁺ channels (18), and transient receptor potential (TRP) channels (19). The polyunsaturated fatty acid arachidonic acid (AA) and its amide anandamide modulate two-pore-domain K⁺ channels (20) and TRP channels (21). Lipid effects on Kv channels, however,

¹Institute of Physiology, University of Freiburg, Hermann-Herder-Straße 7, 79104 Freiburg, Germany.
²Institute of Physiology II, University of Jena, Teichgraben 8, 07744 Jena, Germany.

*These authors contributed equally to this work.
†To whom correspondence should be addressed. E-mail: bernd.fakler@physiologie.uni-freiburg.de (B.F.) and peter.jonas@physiologie.uni-freiburg.de (P.J.)